The ISME Journal (2016) 10, 2715–2724

www.nature.com/ismej

ORIGINAL ARTICLE

Interactions between growth-dependent changes in cell size, nutrient supply and cellular elemental stoichiometry of marine *Synechococcus*

Nathan S Garcia[1], Juan A Bonachela[2] and Adam C Martiny[1,3]
[1]*Department of Earth System Science, University of California, Irvine, CA, USA;* [2]*Department of Mathematics and Statistics, University of Strathclyde, Glasgow, Scotland, UK and* [3]*Department of Ecology and Evolution, University of California, Irvine, CA, USA*

The factors that control elemental ratios within phytoplankton, like carbon:nitrogen:phosphorus (C:N:P), are key to biogeochemical cycles. Previous studies have identified relationships between nutrient-limited growth and elemental ratios in large eukaryotes, but little is known about these interactions in small marine phytoplankton like the globally important Cyanobacteria. To improve our understanding of these interactions in picophytoplankton, we asked how cellular elemental stoichiometry varies as a function of steady-state, N- and P-limited growth in laboratory chemostat cultures of *Synechococcus* WH8102. By combining empirical data and theoretical modeling, we identified a previously unrecognized factor (growth-dependent variability in cell size) that controls the relationship between nutrient-limited growth and cellular elemental stoichiometry. To predict the cellular elemental stoichiometry of phytoplankton, previous theoretical models rely on the traditional Droop model, which purports that the acquisition of a single limiting nutrient suffices to explain the relationship between a cellular nutrient quota and growth rate. Our study, however, indicates that growth-dependent changes in cell size have an important role in regulating cell nutrient quotas. This key ingredient, along with nutrient-uptake protein regulation, enables our model to predict the cellular elemental stoichiometry of *Synechococcus* across a range of nutrient-limited conditions. Our analysis also adds to the *growth rate hypothesis*, suggesting that P-rich biomolecules other than nucleic acids are important drivers of stoichiometric variability in *Synechococcus*. Lastly, by comparing our data with field observations, our study has important ecological relevance as it provides a framework for understanding and predicting elemental ratios in ocean regions where small phytoplankton like *Synechococcus* dominates.
The ISME Journal (2016) **10,** 2715–2724; doi:10.1038/ismej.2016.50; published online 8 April 2016

Introduction

A clear understanding of biogeochemical cycles is key to predicting long-term global change associated with rising atmospheric carbon dioxide (CO_2). The elemental composition of marine phytoplankton is central to ocean biogeochemistry as it links the global carbon (C) cycle with the cycling of other elements, such as nitrogen (N) and phosphorus (P) (Sterner and Elser, 2002; Galbraith and Martiny, 2015). The ratio of elements within organisms is known to vary with energy and nutrient flow through ecosystems (Sterner *et al.*, 1997; Sterner and Elser, 2002; Urabe *et al.*, 2002) and is linked to growth rates and nutritional status. The elemental stoichiometry of biological organisms propagates through the food web to shape community structure and function (Elser *et al.*, 2000) and in turn, marine biota provides a flexible interface, linking global biogeochemical cycles together and can thereby have large effects on climate systems (Finkel *et al.*, 2010; Galbraith and Martiny, 2015). Thus, understanding the factors that influence the elemental stoichiometry of marine organisms is necessary to refine models that forecast how the earth system will change in the future.

Models of biogeochemical cycles traditionally use a fixed ratio of C:N:P for major lineages of marine phytoplankton, although C:N:P of phytoplankton can vary substantially. Countless studies indicate that cellular elemental stoichiometry is highly variable within isolates (Goldman *et al.*, 1979; Geider *et al.*, 1998; Geider and La Roche, 2002) and recent research indicates that C:N:P is also highly variable among ocean regions (Martiny *et al.*, 2013; DeVries and Deutsch, 2014; Teng *et al.*, 2014). Basic knowledge of the underlying physiological mechanisms that control this variability can provide a framework to understand and predict how marine biota interacts with biogeochemical cycles both now and in the future.

Correspondence: AC Martiny, Department of Earth System Science, University of California Irvine, 3208 Croul Hall, Irvine, CA 92697, USA.
E-mail: amartiny@uci.edu
Received 13 October 2015; revised 4 February 2016; accepted 25 February 2016; published online 8 April 2016

Cell models and laboratory studies have examined how multiple factors, such as growth rate and nutrient limitation interact to influence cellular elemental stoichiometry of phytoplankton. Basic physiological mechanisms link growth rates with chemical components within cells, which determine the cellular stoichiometry of elements. For example, the *growth rate hypothesis* (Sterner and Elser, 2002) predicts that ribosomes are needed in high concentrations when cells are growing fast, and the high P-content (~9%) in ribosomal RNA can cause changes in C:P and N:P with growth (Elser *et al*., 2000). Variability in other cell components, such as proteins (Rhee, 1978; Lourenço *et al*., 1998), pigments, phospholipids (Van Mooy *et al*., 2006) and polyphosphates (Rao *et al*., 2009; Martin *et al*., 2014), which are rich in specific elements like N or P, also contribute to variation in cellular elemental stoichiometry and may also co-vary with growth (Rhee 1973). Thus, variable nutrient supply ratios (for example, N:P) are known to influence cellular biochemical content, which can affect growth and elemental stoichiometry of organisms (Rhee, 1978; Goldman *et al*., 1979; Geider and La Roche, 2002; Klausmeier *et al*., 2008).

Related to the *growth rate hypothesis*, empirical data have shown that C:P and N:P of phytoplankton varies when nutrients limit growth (Rhee, 1978; Goldman *et al*., 1979). This relationship has motivated the use of the classic Droop model to predict C:N:P as a function of growth in single- or multiple-nutrient theoretical models (Droop, 1968; Morel, 1987; Legović and Cruzado, 1997; Klausmeier *et al*., 2004a, b; Pahlow and Oschlies, 2009). In the Droop model, the growth rate of an organism increases hyperbolically as the cellular elemental quota of a single, growth-limiting element (for example, P) increases. Klausmeier *et al*. (2004a) used empirical data to build a Droop-based model in which growth rates decline because of decreasing concentrations of a limiting nutrient (for example, NO_3^-), whereas other nutrients that are abundant (for example, PO_4^{3-}) are acquired to store a given element in excess. In other models, phytoplankton elemental stoichiometry results from resource allocation strategies and regulation of nutrient-uptake proteins (Pahlow and Oschlies, 2009; Bonachela *et al*., 2013), which are known to comprise high portions (up to 50%) of cellular N in microbial organisms (Geider and La Roche, 2002). Thus, imbalanced nutrient supplies interact with growth rates to influence the cellular elemental composition through ribosomal RNA, elemental storage and nutrient acquisition mechanisms.

Nearly all of the systematic approaches to studying growth-dependent changes in cellular elemental stoichiometry have focused on large eukaryotic lineages, which are rare or absent from the large oligotrophic gyres throughout the world's oceans. Although some studies have focused on small freshwater phytoplankton including Cyanobacteria (Healey, 1985; Claquin *et al*., 2002; Verspagen *et al*., 2014), less is known about these mechanistic relationships within marine Cyanobacteria, which are known to dominate vast nutrient-poor gyres (Flombaum *et al*., 2013). Recent estimates suggest that they contribute 25% of global marine net primary production and are found in most ocean regions in high abundance (Flombaum *et al*., 2013). Despite their large influence on global biogeochemical cycles, only a few studies have examined the cellular elemental stoichiometry of marine Cyanobacteria (Bertilsson *et al*., 2003; Heldal *et al*., 2003; Ho *et al*., 2003; Finkel *et al*., 2010) and even fewer have focused on physiological mechanisms that may control cellular C:N:P of lineages within Cyanobacteria (Fu *et al*., 2007; Kretz *et al*., 2015; Mouginot *et al*., 2015). Furthermore, none of these studies have examined the well-known interactive influence of growth physiology and nutrient supply on its cellular elemental stoichiometry. These relationships could be different in small phytoplankton in comparison with large phytoplankton, as cell size can reflect important differences in cellular physiology, such as the ability to store nutrients. Knowledge of basic mechanisms that regulate the C:N:P of Cyanobacteria is essential to understand how this globally ubiquitous functional group of primary producers influences ocean biogeochemical cycles and how this influence may change in the future.

Here, we asked how cellular elemental stoichiometry of an isolate of one of the most numerically abundant phytoplankton genera in the global ocean (Flombaum *et al*., 2013), *Synechococcus* (WH8102), varies across a range of N- and P-limited steady-state growth rates in laboratory chemostat cultures. We also evaluated how nucleic acids contribute to cellular elemental stoichiometry by determining how cellular P is biochemically apportioned. Finally, because we documented changes in cell size as a function of growth rate in our chemostat cultures, we used a theoretical model to ask how growth-dependent changes in cell size contributes to relationships between nutrient-limited growth, elemental quotas and cellular elemental stoichiometry. Our results provide a basic understanding of how one of the most abundant marine phytoplankton lineages regulates its elemental composition in the oceans.

Materials and methods

Experiments

Using a modified method from Mouginot *et al*. (2015), cultures of *Synechococcus* (strain WH8102) were grown with a continuous dilution method in 8 l-polycarbonate bottles at 24 °C in an artificial seawater medium at ~195 μmol quanta m^{-2} s^{-1} on a 14:10 light:dark cycle. Light was supplied with cool white fluorescent lamps. We prepared artificial seawater modified from Waterbury and Willey

(1988) (Supplementary Table 1), in 50 l batches before autoclaving 7 l volumes, to which, after cooling, we added 0.2-µm-filter-sterilized carbonates, trace metals, nitrate (NO_3^-) and phosphate (PO_4^{3-}) (Supplementary Table 1). Transfer of media and cultures to the chemostat system were done using a hood and open flame to minimize contamination. The culturing system was enclosed with 0.2 µm-filtered air pumped into the chamber with a 0.2 µm filter attached to an air outlet. We controlled the culture dilution rate and hence the growth rate, by controlling the medium supply rate and the culture volume. The liquid volume in the reservoirs ranged from 2.3 to 5.25 l, thereby yielding a range in dilution rates and steady-state growth rates with equivalent medium input rates. The accumulation of cellular biomass was limited by NO_3^- (added as $NaNO_3$), where measured nutrient concentrations in the medium were 15.9 µM NO_3^- and 9.2 µM PO_4^{3-} (added as K_2HPO_4) yielding a $N:P_{input}$ supply ratio of 1.7, or by PO_4^{3-} with measured concentrations in the medium of 38 µM NO_3^- and 0.56 µM PO_4^{3-}, yielding an $N:P_{input}$ supply ratio of 68. PO_4^{3-} and NO_3^- were measured with a colorimetric assay as described in the Bermuda Atlantic Time-series Methods (Michaels *et al*, 1997a, b) with a spectrophotometer (Genesis 10vis Thermo Scientific, Madison, WI, USA) at 885 and 543 nm, respectively.

Samples from chemostat cultures were collected on pre-combusted 450 °C GF/F filters (Whatman, GE Healthcare, Little Chalfont, Buckinghamshire, UK) for the analysis of particulate organic C and N (200 ml), particulate organic P (50 ml), and DNA and RNA (200 ml). Samples for the analysis of particulate organic C and particulate organic N were dried at 50–80 °C (48+ h), pelletized and analyzed on a Flash EA 1112 NC Soil Analyzer (Thermo Scientific). Samples for the analysis of particulate organic P were rinsed with 0.17 M $NaSO_4$, dried at 60–80 °C with 2 ml of 0.017 M $MgSO_4$, and combusted at 450 °C for 2 h before adding 5 ml 0.2 M HCl and baking at 80–90 °C. The resulting orthophosphate concentrations were measured as described above.

Nucleic acid samples were stored in liquid N until analysis. Cells were lysed with a bead-beater containing 1 ml of a mixed solution containing one part RNA preservation solution (20 mM ethylenediaminetetraacetic acid; 25 mM sodium citrate; and saturated with ammonium sulfate) and four parts 5 mM Tris buffer. Nucleic acids were measured in the supernatant with the Qubit dsDNA HS Assay Kit and the Qubit HS RNA Assay Kit (Invitrogen, Eugene, OR, USA) according to the method described by Zimmerman *et al*. (2014). This technique provides a linear signal in response to the amount of cell material analyzed and is able to recover nearly 100% of material from standards (from Qubit HS Assay Kit) that were spiked into the samples. Cells were counted with an Accuri C6 Flow Cytometer (Ann Arbor, MI, USA) by identifying particles with forward scatter (the proxy flow cytometry estimate for cell size, FSCH) and Chl *a* fluorescence. Fluorescence of phycoerythrin was also determined with the flow cytometer. We estimated cell diameter with a cell–carbon/cell–volume conversion factor calculated with data acquired from a related *Synechococcus* strain (WH8103) growing in artificial seawater (Heldal *et al*., 2003). To summarize trends in steady-state responses to N- and P-limited growth rates, we report the mean and standard deviations on measurements from samples collected on the final three time points of the experimental trials. We fit the Droop model to the growth rate and elemental quota data in Figure 1 using a simple nonlinear least squares method with R statistical software (www.r-project.org) with

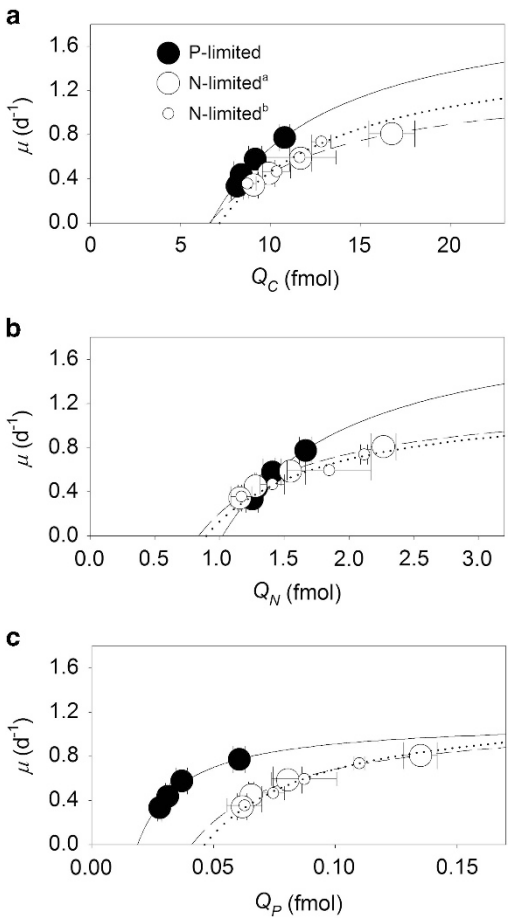

Figure 1 Interactive influence of growth rate and nutrient supply on cellular elemental quotas of *Synechococcus*. Cellular C (Q_C, **a**), N (Q_N, **b**) and P (Q_P, **c**) quotas of *Synechococcus* as a function of steady-state growth (μ) in chemostat cultures limited by nitrate (open symbols) or phosphate (closed symbols). Data were fitted to the Droop model ($\mu = \mu_\infty \cdot [1 - Q'_{min}/Q]$) for P-limited (solid lines), and N-limited (dashed[a] and dotted[b] lines) cells, where μ is the growth rate, μ_∞ is the conditional maximum growth rate, Q'_{min} is the conditional minimum elemental quota and Q is the elemental quota. Large[a] and small[b] open symbols represent data from independent, N-limited culture trials. Standard deviations are plotted on means of triplicate measurements from the last three sampling time points during a trial.

the form $Q = a/(b-\mu)$, where $a = \mu_\infty \cdot Q'_{min}$, $b = \mu_\infty$, Q is elemental quota, and μ is growth rate.

Model

We used the empirical data from the chemostat cultures to expand on an existing model where cellular elemental stoichiometry emerges as a function of the nutrient-limited growth rate (see also Supplementary Information). This model uses physiological foundations similar to other models of cell stoichiometry (Lehman *et al.*, 1975; Bonachela *et al.*, 2013) and includes quota-regulated dynamics that encode changes in the number of nutrient-uptake proteins (Bonachela *et al.*, 2013). These dynamics depend on the quota of the nutrient that is taken up through the so-called *expression* function, *F*, and the P quota (as a proxy for the availability of protein-synthesizing ribosomes) through the *repression* function, *G*. The former encodes protein regulation strategies based on nutrient availability (upregulation for low nutrient, downregulation for high nutrient) (Dyhrman and Palenik, 2001). The latter encodes the feasibility of those strategies based on ribosome availability (for example, low levels of RNA prevent synthesis from happening). For the number of proteins that take up N in the population, n_N, for example, these dynamics are given by the equation:

$$\frac{dn_N}{dt} = \nu_N H(1 - A_{rel}(t)) F\left(\frac{Q_{N_{max}} - Q_N(t)}{Q_{N_{max}} - Q_{N_{min}}}\right) G\left(\frac{Q_P(t) - Q_{P_{min}}}{Q_{P_{max}} - Q_{P_{min}}}\right) B(t) - w n_N(t),$$

where B represents population size, w is the dilution rate of the chemostat, ν_N is the maximum protein synthesis rate per cell and unit time and H is a Heaviside function that depends on the ratio absorbing-to-total area (A_{rel}; that is, a switch that stops protein synthesis when the absorbing area reaches the total area). As explained in the Supplementary Information, n_N is positively correlated with the maximum uptake rate for N; in turn, n_P is positively correlated with the maximum uptake rate for P.

Unlike previous models, however, the maximum and minimum value for the quotas in our model (that is, physiological ranges) are positively correlated with cell size (see Supplementary Information, Equations (18–21)). These expression levels are deduced from our laboratory data. Differently from previous models, we also de-couple the dynamics of population C and population number. Although the dynamics of population C are somewhat controlled by the regulation of photosynthetic proteins (see Supplementary Information, Equation (15)) and other metabolic expenses, the equation for the population number purely depends on cellular quota availability:

$$\frac{dB}{dt} = [f(Q_C, Q_N, Q_P) - w]B(t),$$

where f is a multiplicative function that depends on the three cellular elements. Thus, our expanded model implements variable cellular C quotas. Using different forms for the functional dependence between the C, N and P quotas and the population dynamics of the chemostat cultures, *f*, allowed us to study how the emergent growth rates depend on the shape of this functional dependence (for example, linear or Droop-like hyperbola).

All these components act as a feedback loop. From our chemostat cultures, we were able to deduce that the cellular growth rate influences the maximum C quota and that the cellular C quota influences the maximum and minimum N and P quotas. These extreme quotas are key to the regulation of the nutrient-uptake and photosynthetic proteins, which, in turn, strongly influence nutrients and growth. As the cellular C quota is tightly correlated with cell size, the model ultimately links cell size and growth rate, which influence quota dynamics and elemental stoichiometry. See Supplementary Information for further details.

Results

To understand the interaction between nutrient limitation, growth physiology and cellular elemental stoichiometry, we analyzed steady-state chemostat cultures of *Synechococcus* WH8102 across four growth rates and two different nutrient supply regimes ($N:P_{input} = 1.7$ and $N:P_{input} = 68$). First, we monitored the culture cell density, cell size and particulate organic matter in cultures to ensure they were growing at steady state (Supplementary Figure 1). Both residual dissolved PO_4^{3-} in P-limited cultures and residual dissolved NO_3^- in N-limited cultures were below the detection limit of the spectrophotometric methods used. This indicated that the biomass in cultures, and hence the physiology of cells, were strongly P limited or N limited, respectively (Supplementary Figure 2). In addition, the sum of the residual dissolved PO_4^{3-} and NO_3^- with particulate organic P and particulate organic N concentrations, respectively, were close to measured input concentrations of PO_4^{3-} and NO_3^-. This indicated that cells were able to drawdown nearly all of the PO_4^{3-} or NO_3^- supplied to P-limited or N-limited chemostat cultures, respectively (Supplementary Figure 2). Hence, estimates of culture cell densities, cellular elemental stoichiometry ($C:P_{cell}$ and $N:P_{cell}$) and residual nutrient concentrations suggested that cells had reached a steady state by the end of each chemostat trial (Supplementary Figures 1–3).

Growth rate and culture cell density varied in a negative relationship, with a stronger relationship in P-limited vs N-limited cultures (Supplementary Figures 1A–C). In contrast, the proxy FSCH was positively correlated with the growth rate in steady-state chemostats under both N- and P limitation (Supplementary Figures 1D–F). Throughout each trial, particulate organic C decreased as a function

Table 1 Parameters of the Droop model ($\mu = \mu\infty\ (1-Q'_{min}/Q)$ fit to the data in Figure 1 for N-limited and P-limited cultures of *Synechococcus*

Parameter	*P limited*	*N limited*[a]
Conditional maximum growth rate (day^{-1})		
$\mu_{\infty C}$	2.1 ± 0.1	1.3 ± 0.0, 1.6 ± 0.2
$\mu_{\infty N}$	2.0 ± 0.1	1.3 ± 0.0, 1.3 ± 0.1
$\mu_{\infty P}$	1.1 ± 0.0	1.2 ± 0.0, 1.3 ± 0.0
Conditional minimum quota (fmol cell^{-1})		
$Q'_{C,min}$	6.7 ± 0.7	6.6 ± 0.2, 7.2 ± 1.5
$Q'_{N,min}$	1.0 ± 0.1	0.8 ± 0.02, 0.9 ± 0.2
$Q'_{P,min}$	0.02 ± 0.00	0.04 ± .00, 0.05 ± 0.00
Model fit to quotas		
r^2_C	0.98	0.99, 0.95
r^2_N	0.98	0.99, 0.94
r^2_P	0.99	0.99, 0.99

Abbreviations: C, carbon; N, nitrogen; P, phosphorus.
Variation is reported as the standard error.
[a]Duplicate means represent data from independent N-limited culture trials.

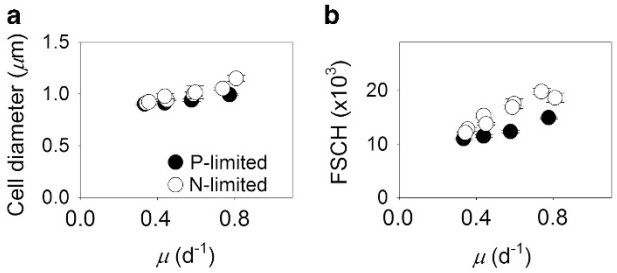

Figure 2 Growth-dependent changes in cell size of *Synechococcus*. Cell size (estimated with a cell C to cell volume relationship) (**a**) and forward scatter (FSCH, a proxy for cell diameter; **b**) of *Synechococcus* cells as a function of steady-state growth (μ) in chemostat cultures limited by nitrate (open symbols) or phosphate (closed symbols). Open circles represent data from two independent, N-limited culture trials. Standard deviations are plotted on means of triplicate measurements from the last three sampling time points during a trial.

of the P-limited growth rate but was relatively invariable under N-limited growth (Supplementary Figures 1G–I).

The steady-state cellular elemental quotas of C, N and P (Q_C, Q_N and Q_P) all increased as a function of growth following a hyperbolic curve resembling the Droop model equation ($r^2 \geq 0.94$, Figure 1 and Table 1). To quantify physiological limits on growth rates and elemental quotas, we defined μ_∞ and Q'_{min} as the conditional maximum growth rate and the conditional minimum elemental quota, respectively, given the ambient light and temperature levels in our experiments. Although the conditional minimum C and N quotas ($Q'_{C,min}$, $Q'_{N,min}$) did not vary between P-limited and N-limited cells (Student's *t*-test, $P > 0.05$, Figure 1a,Table 1), the conditional minimum P quota ($Q'_{P,min}$), significantly increased by 118–146% under N-limited conditions in comparison with P-limited conditions (Figure 1c, Table 1). Also, in P-limited cultures, μ_∞ was significantly higher (Student's *t*-test, $P < 0.05$) when calculated from the Q_C or Q_N data in comparison with that calculated from the Q_P data (Table 1). Collectively, these differences reflect strong differences in the cell quotas as a function of growth and nutrient conditions (Figures 1a–c).

The observed increase in cell quotas with growth rate could lead to changes in overall cell size (Figure 2a). To further examine this, we compared FSCH with growth rates. Growth physiology had a significant effect on FSCH (analysis of covariance test, $F_{1,32} = 239$, $P < 0.001$; Figure 2b). In addition, growth rate and limitation type (N or P) had a significant interactive effect on FSCH (analysis of covariance test, $F_{1,32} = 13$, $P = 0.001$). Thus, N-limited cells were larger than P-limited cells when the growth rate was high (analysis of covariance test, $F_{1,32} = 122$, $P < 0.001$), but the effect of limitation type on FSCH was reduced in slower-growing cells (Figure 2b). We also compared FSCH with other cellular measurements. Cellular nucleic acids (DNA_{cell} and RNA_{cell}, Supplementary Figures 5A and B), pigment fluorescence (fluorescence of Chl *a* and phycoerythrin; Supplementary Figures 4C and D) and cell quotas (Supplementary Figure 4) all varied in a positive linear relationship with FSCH (*t*-test, $P < 0.05$) regardless of limitation type (Supplementary Figure 1). Thus, the effect of growth on cell size was linked to a general increase in cellular mass. Furthermore, the fluorescence of cellular pigments (Chl *a* and phycoerythrin) was elevated under P limitation in comparison with N limitation (analysis of covariance, $F_{1,32} > 9$; $P < 0.05$; Supplementary Figures 4C and D), suggesting an additional effect of limitation type.

We next identified the role of nucleic acids in setting Q_P, as P in RNA has previously been shown to be an important driver of elemental stoichiometry (Sterner and Elser, 2002). First, we observed that the proportion of Q_N in nucleic acids increased as a function of growth under both N- and P limitation, reflecting the general positive relationship between growth and cellular nucleic acid concentrations (Figure 3a, triangles). Despite this positive relationship, the proportion of Q_P devoted to nucleic acids (Figures 3b and c) declined as a function of increasing growth in P-limited cultures ($P < 0.05$; Figure 3a, closed circles). This declining contribution suggested that P-containing cellular resources other than nucleic acids also varied in a positive relationship with P-limited growth. This effect was not observed under N limitation, however, suggesting a tradeoff between non-nucleic acid, P-containing cellular resources or function under N-limited growth (for example, between storage and physiologically active P-containing resources; Figure 3a).

We then identified trends in cellular elemental stoichiometry of *Synechococcus*. $C:P_{cell}$ and $N:P_{cell}$ of *Synechococcus* declined as a linear function with increasing growth (*t*-test, $P < 0.05$; Figures 4a and b)

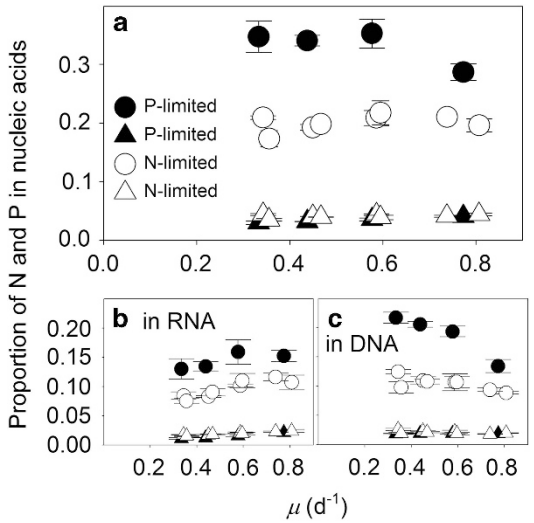

Figure 3 Proportion of cellular N and P quotas devoted to nucleic acids. Cellular N (triangles) and P (circles) in total cellular nucleic acids (**a**), cellular RNA **(b)** and cellular DNA (**c**) as a proportion of total cellular N and P, respectively, as a function of steady-state growth (μ) in chemostat cultures of *Synechococcus* limited by nitrate (open symbols) or phosphate (closed symbols). Open symbols represent data from two independent, N-limited culture trials. Standard deviations are plotted on means of triplicate measurements from the last three sampling time points during a trial.

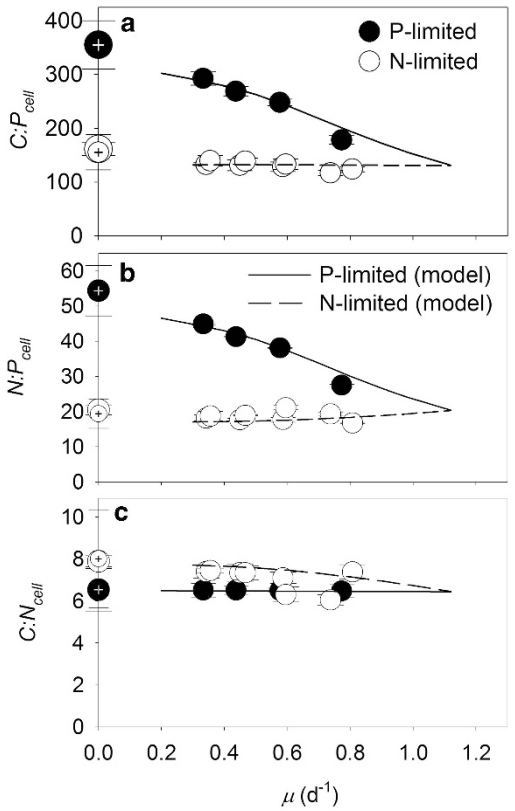

Figure 4 Interactive influence of growth rate and nutrient limitation on cellular stoichiometry of *Synechococcus*. Cellular elemental ratios of C:P ($C:P_{cell}$, **a**), N:P ($N:P_{cell}$, **b**) and C:N ($C:N_{cell}$, **c**) as a function of steady-state growth (μ) in chemostat cultures of *Synechococcus* limited by nitrate (open circles) or phosphate (closed circles). Open circles represent data from two independent, N-limited culture trials. Hashed symbols where $\mu = 0$ represent calculated ratios from conditional minimum elemental quotas (Q'_{min}) from Droop models in Figure 1. Standard deviations are plotted on means of triplicate measurements from the last three sampling time points during a trial. Model output data are also included (see further details in Supplementary Information).

under P limitation. In contrast to the negative linear relationship between $N:P_{cell}$ and P-limited growth, $N:P_{cell}$ was stable under N-limited growth (*t*-test, $P > 0.05$). $C:P_{cell}$ only decreased marginally with N-limited growth (*t*-test, $P < 0.05$, Figure 4b). $C:N_{cell}$ was generally elevated in slow-growing N-limited cultures in comparison with slow-growing P-limited cultures, but was more variable at higher growth rates (Figure 4c). As a result of the strong contrast between our observations, some previous findings, and models of phytoplankton stoichiometry under N limitation, we repeated our N-limited trials with *Synechococcus* and ensured our results could be replicated (Figure 4).

Although the observed behavior of Q_P and Q_N initially mimicked Droop model curves, we were not able to replicate empirical trends in cellular elemental ratios by using existing Droop-based variable quota models nor by using more mechanistic quota-based models with fixed minimum and maximum elemental quota values (Legović and Cruzado, 1997; Klausmeier *et al.*, 2004a). We tested whether the absence of a link between growth-dependent changes in all three elemental quotas and cell size (common to all existing models) is the reason for this failure to replicate our data. Thus, we modified an existing physiological model (Bonachela *et al.*, 2013) to include growth-dependent changes in cell size that influence cellular elemental quotas as well as their maximum and minimum values, which in turn are key in the regulation of nutrient-uptake proteins (see Supplementary Information). Our expanded model captures the observed relationship between cellular elemental stoichiometry and growth (Figure 4) including the 'Droop-like' behavior for all cellular elemental quotas. Only the inclusion of growth-dependent cell size and quota-dependent protein regulation enabled the replication of the observed behavior. Importantly, these two key underlying mechanisms are fundamentally different than those in the Droop model, and confirm the strong influence of cell size on the resulting cellular elemental quotas and ratios.

Discussion

Using controlled chemostat cultures of an isolate representing one of the most abundant marine phytoplankton lineages, we observed strong inconsistencies between our data and some fundamental conceptual mechanisms that have commonly been invoked to understand the elemental composition of phytoplankton. First, although RNA_{cell} and DNA_{cell} increased with increasing growth rate, thereby supporting a key aspect of the growth rate hypothesis

(Sterner and Elser, 2002), the proportion of Q_P devoted to nucleic acids did not increase with increasing growth, suggesting that P in nucleic acids is not the central driver of the cellular elemental stoichiometry of *Synechococcus* within this growth rate range. Our estimates of this proportion agree with previous estimates indicating that RNA_{cell} is low in *Synechococcus* (Mouginot *et al.*, 2015) and imply that P-rich biomolecules other than nucleic acids also co-vary with growth (Figure 3). Nucleic acids may have a more dominant influence when growth rates are very close to μ_{max}, however, and in absence of μ_{max} data for WH8102, our high growth rate cultures represent ~67–73% of μ_{max} of a related isolate of *Synechococcus* (Moore *et al.*, 1995). Nucleic acids may also have a stronger influence on stoichiometric differences across lineages where maximum growth rates are vastly different (Elser *et al.*, 2000), rather than within a single isolate.

A second departure from the accepted conceptual models of cellular elemental stoichiometry is the observed role of cell size and associated quotas as a function of growth. Although none of the previous theoretical models include growth-dependent variability in cell size, our data indicate that cell size and all of the cell components that we measured (Q_C, Q_N, Q_P, DNA_{cell}, RNA_{cell} and cellular pigment fluorescence) were positively related to the cellular growth rate (Figure 2, Supplementary Figures 4 and 5). Cell size is a critical ingredient in our expanded model of cellular elemental stoichiometry because it allows Q_C, Q_N and Q_P to change as a function of growth, however, disproportionately. In support of this, some previous data acknowledge growth-dependent changes in cell size of phytoplankton (Cook, 1963). The positive relationship between cell size and growth rate is a common observation within specific isolates of microbes and has been termed the *growth rate law* (Schaechter *et al.*, 1958; Vadia and Levin, 2015). However, Q_C or cell size has typically been held constant under variable growth rates in previous theoretical models (for example,, Shuter, 1979; Klausmeier *et al.*, 2008; Bonachela *et al.*, 2013). Instead, theoretical models typically rely on the Droop model equation to describe growth-dependent relationships in the ratios of cellular elements.

Although the Droop model equation fits our Q_N and Q_P data well, the model's underlying mechanism is fundamentally different than the cell size–growth rate relationship. The traditional Droop model focuses on growth-dependent changes in a single growth-limiting elemental quota (such as Q_N or Q_P), whereas our data demonstrate that the cell size–growth relationship contributes to growth-dependent changes in all three of the cellular elemental quotas that we measured. For example, the Droop model fits our Q_C data very well, but this fit did not result from C limitation, as the Droop model would predict. Instead, changes in Q_C were directly related to growth-dependent changes in cell size, and the Droop model coincidentally fit these changes in cell size. This is also evident from our Q_N data, which follow the Droop model relationship in contrasting P-limited chemostats. Under P-limited growth, nitrate was in high abundance but Q_N fit the Droop model in nearly the same way as N-limited cells (Figure 1b). Therefore, the Droop model fits to Q_N and Q_P do not result directly from N or P acquisition, but instead, as our model confirms, result from the cell size–growth rate relationship. Thus, by decoupling the equations for the population C and number of cells, we achieved a dynamic regulation of Q_C (and hence a cell size–growth rate link), which together with the dynamics of Q_N and Q_P and their effect on protein regulation, was necessary to predict our observed trends in cellular elemental stoichiometry of *Synechococcus*.

In contrast with Droop-based models of phytoplankton stoichiometry, where $C:P_{cell}$ and $N:P_{cell}$ change sharply as a function of P-limited growth (Klausmeier *et al.*, 2004b; Bonachela *et al.*, 2013), our model and data indicate that $C:P_{cell}$ and $N:P_{cell}$ of *Synechococcus* decrease almost linearly as a function of P-limited growth (Figures 4a and b). We also obtained marginal changes in $C:P_{cell}$ and no change in $N:P_{cell}$ as a function of N-limited growth, and collectively, these trends have been observed previously in other phytoplankton (Goldman *et al.*, 1979). The invariable $N:P_{cell}$ under N-limited growth is remarkable for the globally abundant *Synechococcus* because $N:P_{cell}$ is consistently close to the Redfield ratio (16) even under severe N limitation, a common state among field populations (Moore *et al.*, 2013). Understanding environmental controls on cellular elemental stoichiometry in the small but dominant prokaryotic phytoplankton lineages under N limitation may be key to understanding the primary drivers of Redfield stoichiometry in the oceans. But the mechanisms that contribute to variability in cellular elemental stoichiometry may be different for different lineages because this invariable trend does not appear to be consistent across lineages of phytoplankton (Goldman *et al.*, 1979).

We also observed moderate decreases in $C:N_{cell}$ under severely P-limited growth in comparison with severely N-limited growth, which seem to be related to cell size and pigment fluorescence (Figure 4). N-limited cells were larger than P-limited cells, evident from differences in FSCH (Figure 2) and Q_C (Figure 1a) between these two treatments. Despite differences in cell size, Q_N was relatively invariable between N- and P-limited cells (Figure 1b). This generally resulted in elevated $C:N_{cell}$ in slow-growing N-limited cells in comparison with other treatments (Figure 4c), which, based on our pigment fluorescence data, seems to be caused by higher cellular concentrations of N-rich pigments in P-limited cells (Supplementary Figures 5C and D). As phycoerythrin, a dominant pigment in *Synechococcus* (Scanlan *et al.*, 2009), is composed of protein, and proteins comprise a large portion of Q_N (Rhee, 1978; Lourenço *et al.*, 1998), the rigidity in Q_N between P- and

N-limited cells may be caused by differences in phycoerythrin, which is known to have a dual role in photosynthesis and N storage (Wyman *et al.*, 1985; Yeh *et al.*, 1986). Thus, the decline in $C:N_{cell}$ in severely P-limited cells seems to result from the combined effect of smaller cells and higher pigment fluorescence in comparison with severely N-limited cells.

In general, small phytoplankton are thought to lack major nutrient storage reservoirs. Aside from small differences in cellular pigment fluorescence, we did not observe signs of abundant N or P storage in *Synechococcus*. Some theoretical models rely on cellular storage components to predict cellular stoichiometry (Daines *et al.*, 2014), but our observed changes in Q_N with growth were mainly dependent on changes in cell size, regardless of limitation type. This observation is consistent with the general lack of the major N storage compound—cyanophycin—in *Synechococcus* isolates (Wingard *et al.*, 2002). In models, Q_N or Q_P increases as a function of decreasing growth in environments, where N or P is abundant, respectively (that is, where P or N is limiting growth, respectively) (Klausmeier *et al.*, 2004b, 2008). Although pigments probably contributed to minor N storage under slow P-limited growth, the large increases in $N:P_{cell}$ (Figure 4b) in our experiments did not result from abundant increases in cellular N storage, as Q_N was roughly linked to cell volume (Supplementary Figure 6A, closed symbols). Instead, the strong variation in $N:P_{cell}$ as a function of P-limited growth (Figure 4b) resulted from stronger changes in Q_P (Figure 1c) relative to moderate changes in cell size (that is, Q_C) (Figure 1a) and relative to small changes in Q_N under N limitation. Even under slow N-limited growth, cells did not store P in high excess either; changes in Q_P in P-replete environments were also tightly linked to changes in cell volume (Supplementary Figure 6B, open symbols). Thus, the major variation in $C:P_{cell}$ and $N:P_{cell}$ within *Synechococcus* (Figures 4a and b) seems to be driven by a larger percent change in Q_P relative to percent changes in cell size (Q_C) and Q_N under P-limited growth, in comparison with small percent changes in Q_N relative to changes in cell size (Q_C) and Q_P under N-limited growth. But we did not observe drastic increases in Q_P or Q_N under different N- or P-limited environments as modeled previously (Klausmeier *et al.*, 2004a), indicating that N and P were not stored in high abundance in N- or P-replete environments, respectively.

In consideration of how $C:P_{cell}$ and $N:P_{cell}$ varies relative to cell size (Q_C) and Q_N in P- and N-limited environments, we postulate that variable cell concentrations of P-rich biomolecules must be major drivers of stoichiometric variation in *Synechococcus*. Cellular phospholipid concentrations are known to decline under P limitation (Van Mooy *et al.*, 2006) but in general do not represent a large proportion of cellular P (Mouginot *et al.*, 2015). Although much less is known about polyphosphates in Cyanobacteria, they may also co-vary with growth in *Synechococcus*, as documented in another species of phytoplankton (Rhee, 1973). Although some data suggest that the adenylate pool increased with increasing growth rate in heterotrophic bacteria (Marriot *et al.*, 1981), adenosine triphosphate in *Synechococcus* WH8102 was highly correlated with FSCH regardless of the chemostat dilution rate and represented $<1\%$ of Q_P in another experiment (unpublished data). The general lack of major storage reservoirs in small Cyanobacteria may be key to distinguishing trends in cellular elemental stoichiometry from those in larger phytoplankton, as previous data with diatoms suggest that Q_C increases with decreasing P-limited growth (Laws and Bannister, 1980), contrasting the diminishing Q_C with decreasing growth of *Synechococcus* (Figure 1a).

Ecological implications

Our results may be applied to broadly understand the physiological status of unicellular Cyanobacteria in the ocean. If we compare our results with stoichiometric data compiled by Martiny *et al.* (2013) and inversely estimated by Teng *et al.* (2014), the high C:P ratios observed in the P-limited North Atlantic Subtropical Gyre (Moore *et al.*, 2009; Lomas *et al.*, 2010) are congruent with $C:P_{cell}$ of *Synechococcus* when growth rates are strongly P limited. In contrast, the moderate C:P ratios (but above Redfield proportions) observed in the presumed N-limited Southern Atlantic Subtropical Gyre (Teng *et al.*, 2014) are similar to the C:P ratios that we observed in slower-growing N-limited cultures. The low C:P estimates in the eastern equatorial Atlantic upwelling region (where nutrients are abundant) are consistent with a high frequency of fast-growing *Synechococcus* cells. Thus, our data and model seem to corroborate the physiological status of biota in major ocean basins and our observations suggest that the growth-dependent variability in cell size and the lack of elemental storage capacity both influence the cellular elemental stoichiometry of small marine phytoplankton within field populations. In comparison with data collected from other species of phytoplankton, our findings further suggest that fundamentally different biochemical mechanisms may control the cellular elemental stoichiometry of small vs large phytoplankton, such as Cyanobacteria vs eukaryotes. Such biochemical mechanisms can contribute to understanding broad scale patterns in ocean biogeochemistry and regional differences in C:N:P. As studies of environmental controls on cellular elemental stoichiometry emerge among broader lineages of phytoplankton, we may begin to forecast how ocean biogeochemical cycles will respond to global change.

Conflict of Interest

The authors declare no conflict of interest.

Acknowledgements

Support for this research was provided by the UCI Chancellor's ADVANCE Postdoctoral Program and the National Science Foundation Dimensions of Biodiversity (OCE-1046297) and Major Research Instrumentation programs (OCE-1126749). JAB acknowledges support of the MASTS pooling initiative (The Marine Alliance for Science and Technology for Scotland). MASTS is funded by the Scottish Funding Council (grant reference HR09011) and contributing institutions.

References

Bertilsson S, Berglund O, Karl DM, Chisholm SW. (2003). Elemental composition of marine *Prochlorococcus* and *Synechococcus*: Implications for the ecological stoichiometry of the sea. *Limnol Oceanogr* **48**: 1721–1731.

Bonachela JA, Allison SD, Martiny AC, Levin SA. (2013). A model for variable phytoplankton stoichiometry based on cell protein regulation. *Biogeosciences* **10**: 4341–4356.

Claquin P, Martin-jézéquel V, Kromkamp JC, Veldhuis MJW, Kraay GW. (2002). Uncoupling of silicon compared with carbon and nitrogen metabolisms and the rol of the cell cycle in continuous cultures of *Thalassiosira pseudonana* (Bacillariophyceae) under light, nitrogen, and phosphorus control. *J Phycol* **38**: 922–930.

Cook JR. (1963). Adaptations in growth and division in euglena effected by energy supply. *J Protozool* **10**: 436–444.

Daines SJ, Clark JR, Lenton TM. (2014). Multiple environmental controls on phytoplankton growth strategies determine adaptive responses of the N : P ratio. *Ecol Lett* **17**: 414–425.

DeVries T, Deutsch C. (2014). Large-scale variations in the stoichiometry of marine organic matter respiration. *Nat Geosci* **7**: 890–894.

Droop MR. (1968). Vitamin B_{12} and marine ecology. IV. The kinetics of uptake, growth and inhibtition in *Monochrysis lutheri*. *J Mar Biol Ass UK* **48**: 689–733.

Dyhrman ST, Palenik B. (2001). A single-cell immunoassay for phosphate stress in the dinoflagellate *Prorocentrum minimum* (Dinophyceae). *J Phycol* **37**: 400–410.

Elser JJ, O'Brien WJ, Dobberfuhl DR, Dowling TE. (2000). The evolution of ecosystem processes: growth rate and elemental stoichiometry of a key herbivore in temperate and arctic habitats. *J Evol Biol* **13**: 845–853.

Elser JJ, Sterner RW, Gorokhova E, Fagan WF, Markow TA, Cotner JB *et al.* (2000). Biological stoichiometry from genes to ecosystems. *Ecol Lett* **3**: 540–550.

Finkel ZV, Beardall J, Flynn KJ, Quigg A, Rees TAV, Raven JA. (2010). Phytoplankton in a changing world: cell size and elemental stoichiometry. *J Plankton Res* **32**: 119–137.

Flombaum P, Gallegos JL, Gordillo RA, Rincón J, Zabala LL, Jiao N *et al.* (2013). Present and future global distributions of the marine Cyanobacteria *Prochlorococcus* and *Synechococcus*. *Proc Natl Acad Sci USA* **110**: 9824–9829.

Fu FX, Warner ME, Zhang Y, Feng Y, Hutchins DA. (2007). Effects of increased temperature and CO_2 on photosynthesis, growth, and elemental ratios in marine *Synechococcus* and *Prochlorococcus* (Cyanobacteria). *J Phycol* **43**: 485–496.

Galbraith ED, Martiny AC. (2015). A simple nutrient-dependence mechanism for predicting the stoichiometry of marine ecosystems. *Proc Natl Acad Sci USA* **112**: 201423917.

Geider R, La Roche J. (2002). Redfield revisited: variability of C:N:P in marine microalgae and its biochemical basis. *Eur J Phycol* **37**: 1–17.

Geider RJ, MacIntyre HL, Kana TM. (1998). A dynamic regulatory model of phytoplanktonic acclimation to light, nutrients, and temperature. *Limnol Oceanogr* **43**: 679–694.

Goldman JC, McCarthy JJ, Peavey DG. (1979). Growth rate influence on the chemical composition of phytoplankton in oceanic waters. *Nature* **279**: 210–215.

Healey F. (1985). Interacting effects of light and nutrient limitation on the growth rate of *Synechococcus linearis* (Cyanophyceae). *J Phycol* **21**: 134–146.

Heldal M, Scanlan DJ, Norland S, Thingstad F, Mann NH. (2003). Elemental composition of single cells of various strains of marine *Prochlorococcus* and *Synechococcus* using X-ray microanalysis. *Limnol Oceanogr* **48**: 1732–1743.

Ho T-Y, Quigg A, Finkel ZV, Milligan AJ, Wyman K, Falkowski PG *et al.* (2003). The elemental composition of some marine phytoplankton. *J Phycol* **39**: 1145–1159.

Klausmeier CA, Litchman E, Daufresne T, Levin SA. (2004a). Optimal nitrogen-to-phosphorus stoichiometry of phytoplankton. *Nature* **429**: 171–174.

Klausmeier CA, Litchman E, Daufresne T, Levin SA. (2008). Phytoplankton stoichiometry. *Ecol Res* **23**: 479–485.

Klausmeier CA, Litchman E, Levin SA. (2004b). Phytoplankton growth and stoichiometry under multiple nutrient limitation. *Limnol Oceanogr* **49**: 1463–1470.

Kretz CB, Bell DW, Lomas DA, Lomas MW, Martiny AC. (2015). Influence of growth rate on the physiological response of marine *Synechococcus* to phosphate limitation. *Front Microbiol* **6**: 6–11.

Laws EA, Bannister TT. (1980). Nutrient- and light-limited growth of *Thalassiosira fluviatilis* in continuous culture, with implications for phytoplankton growth in the ocean. *Limnol Oceanogr* **25**: 457–473.

Legović T, Cruzado A. (1997). A model of phytoplankton growth on multiple nutrients based on the Michaelis-Menten-Monod uptake, Droop's growth and Liebig's law. *Ecol Modell* **99**: 19–31.

Lehman JT, Botkin DB, Likens GE. (1975). The assumptions and rationales of a computer model of phytoplankton dynamics. *Limnol Oceanogr* **20**: 343–364.

Lomas MW, Burke AL, Lomas DA, Bell DW, Shen C, Dyhrman ST *et al.* (2010). Sargasso Sea phosphorus biogeochemistry: an important role for dissolved organic phosphorus (DOP). *Biogeosciences* **7**: 695–710.

Lourenço SO, Barbarino E, Marquez UML, Aidar E. (1998). Distribution of intracellular nitrogen in marine microalgae: Basis for the calculation of specific nitrogen-to-protein conversion factors. *J Phycol* **34**: 798–811.

Marriot ID, Edwin AD, Rowley BI. (1981). Effect of growth rate and nutrient limitation on the adenine nucleotide content, energy charge and enzymes of adenylate metabolism in *Azotobacter beijerinckii*. *J Gen Microbiol* **125**: 375–382.

Martin P, Dyhrman ST, Lomas MW, Poulton NJ, Van Mooy BAS. (2014). Accumulation and enhanced

cycling of polyphosphate by Sargasso Sea plankton in response to low phosphorus. *Proc Natl Acad Sci USA* **111**: 8089–8094.

Martiny AC, Pham CTA, Primeau FW, Vrugt JA, Moore JK, Levin SA *et al.* (2013). Strong latitudinal patterns in the elemental ratios of marine plankton and organic matter. *Nat Geosci* **6**: 279–283.

Michaels A, Dow R, Elardo K. (1997a). The determination of phosphorus in seawater. In: *Bermuda Atlantic Time-Series Study Methods*. JGOFS Planning Office: Woods Hole, MA, USA, pp 71–74.

Michaels A, Dow R, Howse F. (1997b). The determination of nitrate in seawater. In: *Bermuda Atlantic Time-series Study Methods*. JGOFS Planning Office: Woods Hole, MA, USA, pp 61–66.

Moore CM, Mills MM, Achterberg EP, Geider RJ, LaRoche J, Lucas MI *et al.* (2009). Large-scale distribution of Atlantic nitrogen fixation controlled by iron availability. *Nat Geosci* **2**: 867–871.

Moore CM, Mills MM, Arrigo KR, Berman-Frank I, Bopp L, Boyd PW *et al.* (2013). Processes and patterns of oceanic nutrient limitation. *Nat Geosci* **6**: 701–710.

Moore LR, Goericke R, Chisholm S. (1995). Comparative physiology of *Synechococcus* and *Prochlorococcus*: influence of light and temperature on the growth, pigments, fluorescence and absorptive properties. *Mar Ecol Prog Ser* **116**: 259–275.

Morel FMM. (1987). Kinetics of nutrient uptake and growth in phytoplankton. *J Phycol* **23**: 137–150.

Mouginot C, Zimmerman AE, Bonachela JA, Fredricks H, Allison SD, Van Mooy BAS *et al.* (2015). Resource allocation by the marine cyanobacterium *Synechococcus* WH8102 in response to different nutrient supply ratios. *Limnol Oceanogr* **60**: 1634–1641.

Pahlow M, Oschlies A. (2009). Chain model of phytoplankton P, N and light colimitation. *Mar Ecol Prog Ser* **376**: 69–83.

Rao NN, Gómez-García MR, Kornberg A. (2009). Inorganic polyphosphate: essential for growth and survival. *Annu Rev Biochem* **78**: 605–647.

Rhee GY. (1978). Effects of N:P atomic ratios nitrate limitation on algal growth, cell composition, nitrate uptake. *Limnol Oceanogr* **23**: 10–25.

Rhee G-Y. (1973). A continuous culture study of phosphate uptake, growth rate, and polyphosphate in *Scenedesmus* sp. *J Phycol* **9**: 495–506.

Scanlan DJ, Ostrowski M, Mazard S, Dufresne A, Garczarek L, Hess WR *et al.* (2009). Ecological genomics of marine picocyanobacteria. *Microbiol Mol Biol Rev* **73**: 249–299.

Schaechter M, MaalOe O, Kjeldgaard NO. (1958). Dependency on medium and temperature of cell size and chemical composition during balanced growth of *Salmonella typhimurium*. *J Gen Microbiol* **19**: 592–606.

Shuter B. (1979). A model of physiological adaptation in unicellular algae. *J Theor Biol* **78**: 519–552.

Sterner RW, Elser JJ. (2002). *Ecological Stoichiometry: The Biology of Elements from Molecules to the Biosphere*. Princeton University Press: Princeton, NJ, USA.

Sterner RW, Elser JJ, Fee EJ, Guildford SJ, Chrzanowski TH. (1997). The light: nutrient ratio in lakes: the balance of energy and materials affects ecosystem structure and process. *Am Nat* **150**: 663–684.

Teng Y-C, Primeau FW, Moore JK, Lomas MW, Martiny AC. (2014). Global-scale variations of the ratios of carbon to phosphorus in exported marine organic matter. *Nat Geosci* **7**: 895–898.

Urabe J, Kyle M, Makino W, Yoshida T, Andersen T, Elser JJ. (2002). Reduced light increases herbivore production due to stoichiometric effects of light/nutrient balance. *Ecology* **83**: 619–627.

Vadia S, Levin PA. (2015). Growth rate and cell size: a re-examination of the growth law. *Curr Opin Microbiol* **24**: 96–103.

Van Mooy BAS, Rocap G, Fredricks HF, Evans CT, Devol AH. (2006). Sulfolipids dramatically decrease phosphorus demand by picocyanobacteria in oligotrophic marine environments. *Proc Natl Acad Sci USA* **103**: 8607–8612.

Verspagen JMH, Van de Waal DB, Finke JF, Visser PM, Huisman J. (2014). Contrasting effects of rising CO_2 on primary production and ecological stoichiometry at different nutrient levels. *Ecol Lett* **17**: 951–960.

Waterbury J, Willey JM. (1988). Isolation and growth of marine planktonic Cyanobacteria. *Methods Enzymol* **167**: 100–105.

Wingard LL, Miller SR, Sellker JML, Stenn E, Allen MM, Wood A M. (2002). Cyanophycin production in a phycoerythrin-containing marine *Synechococcus* strain of unusual phylogenetic affinity. *Appl Environ Microbiol* **68**: 1772–1777.

Wyman M, Gregory RP, Carr NG. (1985). Novel role for phycoerythrin in a marine cyanobacterium, *Synechococcus* strain DC2. *Science* **230**: 818–820.

Yeh SW, Ong LJ, Glazer AN. (1986). Role of phycoerythrin in marine picoplankton *Synechococcus* spp. *Science* **234**: 1422–1423.

Zimmerman AE, Allison SD, Martiny AC. (2014). Phylogenetic constraints on elemental stoichiometry and resource allocation in heterotrophic marine bacteria. *Environ Microbiol* **16**: 1398–1410.

Supplementary Information accompanies this paper on The ISME Journal website (http://www.nature.com/ismej)